# Present Status of Inflation after WMAP and SDSS data

**Yong-Yeon Keum**

Feburary 10-12, 2009

*SDSS-KSG Winter-Workshop*

# Outline

# Introduction:

Inflation was introduced to solve several outstanding problems of the Standard Big-Bang model:

- Horizon problem
- Flatness problem
- Homogeneity and Isotropy Problem

Now it has become an important part of the Standard Cosmology.

Inflation models not only explain the large-scale homogeneity of the unverse, but also provide a mechanism for explaining the observed level of inhomogeneity as well.

## Present Status:

The metric perturbations created during inflation are of two types: scalar and tensor:

⇒ provided a natural mechanism for

- the generation of scalar density fluctuations that seed of large scale structure (curvature perturbation),
- the generation of tensor perturbation (Primordial gravitational waves).

A great diversity of inflationary models predict:
fairly generic features:

- Gaussian
- Nearly scale invariant spectrum of adiabatic scalar and tensor primordial fluctuations

⇒ provide an excellent fit to the highly precise wealth of data from WMAP.

# Single-Field Inflation

The evolution of a Friedmann-Robertson-Walker (FRW) universe dominated by a single minimally-coupled scalar field (the *inflaton*)

$$H^2 = \frac{8\pi}{3m_{\rm Pl}^2}\left[\frac{1}{2}\dot{\phi}^2 + V(\phi)\right], \quad (1)$$

$$\frac{\ddot{a}}{a} = \frac{8\pi}{3m_{\rm Pl}^2}\left[V(\phi) - \dot{\phi}^2\right]. \quad (2)$$

Here the metric $g_{\mu\nu} = \mathrm{diag}(1, -a^2, -a^2, -a^2)$, where $a(t)$ is the scale factor and dots denote derivatives with respect to coordinate time, $t$.
The evolution of the scalar field follows:

$$\ddot{\phi} + 3H\dot{\phi} + V' = 0, \quad (3)$$

where primes denote derivatives with respect to the field, $\phi$.

## Single-Field Inflation

Equations (1) and (3) can be combined to yield the alternative equations of motion,

$$\dot{\phi} = -\frac{m_{\rm Pl}^2}{4\pi} H'(\phi), \tag{4}$$

$$H'(\phi)^2 - \frac{12\pi}{m_{\rm Pl}^2} H^2(\phi) = -\frac{32\pi^2}{m_{\rm Pl}^4} V(\phi), \tag{5}$$

where the Hubble parameter, written as a function of $\phi$, becomes the dynamical variable.
The second of the above two equations is known as the *Hamilton-Jacobi equation*, and may be written more simply as

$$H^2(\phi)\left[1 - \frac{1}{3}\epsilon(\phi)\right] = \left(\frac{8\pi}{3m_{\rm Pl}^2}\right) V(\phi), \tag{6}$$

where the parameter $\epsilon$ is defined as

$$\epsilon = \frac{m_{\rm Pl}^2}{4\pi}\left(\frac{H'(\phi)}{H(\phi)}\right)^2, \qquad \left(\frac{\ddot{a}}{a}\right) = H^2(\phi)\left[1 - \epsilon(\phi)\right], \tag{7}$$

Physically, $\epsilon$ is the equation-of-state parameter of the cosmological fluid, and the condition for inflation, $\ddot{a} > 0$, requires that $\epsilon < 1$.

## Single-Field Inflation

Starting with the equation-of-state parameter, it is possible to define an infinite hierarchy of parameters by taking successive derivatives of the Hubble parameter, $H(\phi)$,

$$\epsilon = \frac{m_{\rm Pl}^2}{4\pi}\left(\frac{H'(\phi)}{H(\phi)}\right)^2 \simeq \frac{m_{\rm Pl}^2}{16\pi}\left(\frac{V'(\phi)}{V(\phi)}\right)^2, (EoS) \qquad (8)$$

$$\eta = \frac{m_{\rm Pl}^2}{4\pi}\left(\frac{H''(\phi)}{H(\phi)}\right) \simeq \frac{m_{\rm Pl}^2}{8\pi}\left[\frac{V''(\phi)}{V(\phi)} - \frac{1}{2}\left(\frac{V'(\phi)}{V(\phi)}\right)^2\right], \qquad (9)$$

$$\xi^2 = \frac{m_{\rm Pl}^4}{(4\pi)^2}\left(\frac{H'(\phi)H'''(\phi)}{H^2(\phi)}\right),$$

$$\vdots$$

$${}^n\lambda_H = \left(\frac{m_{\rm Pl}^2}{4\pi}\right)^n \frac{(H'(\phi))^{n-1}}{H^n(\phi)}\frac{d^{(n+1)}H}{d\phi^{(n+1)}}.$$

In what follows, we will refer to Eqs. (7) and (8) collectively as the *Hubble flow parameters*. These are often referred to as *slow-roll* parameters in the literature, however, they are defined here without any assumption of slow-roll.

## Single-Field Inflation

The scale factor may be written ($a \propto e^N$, ): N=number of e-fold and from Eq. (1),

$$dN = -Hdt = \frac{H}{\dot{\phi}} d\phi = \frac{2\sqrt{\pi}}{m_{\rm Pl}} \frac{d\phi}{\sqrt{\epsilon(\phi)}}. \qquad (10)$$

Making use of this relation, we take successive derivatives of the flow parameters with respect to $N$, generating an infinite set of differential equations,

$$\begin{aligned} \frac{dH}{dN} &= \epsilon H, \\ \frac{d\epsilon}{dN} &= \epsilon(\sigma + 2\epsilon), \\ \frac{d\sigma}{dN} &= -5\epsilon\sigma - 12\epsilon^2 + 2\xi^2, \\ \frac{d({}^\ell\lambda_H)}{dN} &= \left[\frac{\ell - 1}{2}\sigma + (\ell - 2)\epsilon\right]({}^\ell\lambda_H) + {}^{\ell+1}\lambda_H, \end{aligned} \qquad (11)$$

where $\sigma = 2\eta - 4\epsilon$. In practice, this system is truncated at some finite order $M$ by requiring that ${}^{M+1}\lambda_H = 0$.

# Single-Field Inflation

This system can then be solved numerically by specifying the initial conditions of the parameters $\epsilon$, $\sigma, \ldots, {}^{M}\lambda_H$ at some arbitrary time, $N_i$. Although the system is truncated at finite order, this results in an *exact* solution for the background evolution of an FRW universe dominated by a single scalar field. This is due to the form of the flow equations, where it can be seen that the truncation ${}^{M+1}\lambda_H = 0$ ensures that all higher-order parameters vanish for all time. The initial conditions were drawn randomly from the ranges

$$\begin{aligned} N &\in [46, 60] \\ \epsilon &\in [0, 0.8] \\ \sigma &\in [-0.5, 0.5] \\ \xi^2 &\in [-0.05, 0.05] \\ {}^{3}\lambda_H &\in [-0.005, 0.005] \\ &\vdots \\ {}^{M+1}\lambda_H &\in 0, \end{aligned} \qquad (12)$$

although other choices are possible.

# Single-Field Inflation

The values of the flow parameters at $N_{obs}$ can then be used to calculate observables via the relations:

$$
\begin{aligned}
r &= 16\epsilon[1 - C(\sigma + 2\epsilon)], \\
n_s &= 1 + \sigma - (5 - 3C)\epsilon^2 \\
&\quad -\frac{1}{4}(3 - 5C)\sigma\epsilon + \frac{1}{2}(3 - C)\xi^2, \\
\alpha &= \frac{dn_s}{d\ln k} = -\left(\frac{1}{1-\epsilon}\right)\frac{dn_s}{dN},
\end{aligned}
\tag{13}
$$

where $C = 4(\ln 2 + \gamma) - 5$, $\gamma \simeq 0.577$.

## Inflationary Observables

- The comoving curvature perturbation $P_{\mathcal{R}}$:

$$P_{\mathcal{R}}^{1/2}(k) = \left(\frac{H^2}{2\pi\dot{\phi}}\right)_{k=aH} = \left[\frac{H}{m_{\rm Pl}}\frac{1}{\sqrt{\pi\epsilon}}\right]_{k=aH}. \qquad (14)$$

- The power spectrum of tensor fluctuation modes is given:

$$P_T^{1/2}(k_N) = \left[\frac{4H}{m_{\rm Pl}\sqrt{\pi}}\right]_N. \qquad (15)$$

- The *spectral index* $n$ for $P_{\mathcal{R}}$ is defined:

$$n - 1 \equiv \frac{d\ln P_{\mathcal{R}}}{d\ln k}, \qquad (16)$$

- The ratio of tensor-to-scalar modes is then $P_T/P_{\mathcal{R}} = 16\epsilon$, so that tensor modes are negligible for $\epsilon \ll 1$.

A given inflation model can be described to lowest order by three independent parameters, $P_{\mathcal{R}}$, $P_T$, and $n$. Including higher-order effects, we have a fourth parameter describing the running of the scalar spectral index, $dn/d\ln k$.

# Inflationary Observables

Generally well approximated by power laws:

$$P_{\mathcal{R}}(k) \propto k^{n-1}, \qquad P_T(k) \propto k^{n_T}. \tag{17}$$

In the limit of slow roll, the spectral indices $n$ and $n_T$ vary slowly or not at all with scale. We can write the spectral indices $n$ and $n_T$ to lowest order in terms of the slow roll parameters $\epsilon$ and $\eta$ as:

$$\begin{aligned} n &\simeq 1 - 4\epsilon + 2\eta, \\ n_T &\simeq -2\epsilon = -\frac{r}{8}. \end{aligned} \tag{18}$$

The tensor/scalar ratio is frequently expressed as a quantity $r$, which is conventionally normalized as

$$r \equiv 16\epsilon = \frac{P_{\rm T}}{P_{\mathcal{R}}}. \tag{19}$$

# Analysis Method

- Calculating the CMB-fluctuations from a particular inflation model:
  - From the potential, calculate $\epsilon$ and $\eta$.
  - From $\epsilon$, calculate $N$ as a function of the field $\phi$.
  - Invert $N(\phi)$ to find $\phi_N$.
  - Calculate $P_{\mathcal{R}}$, $n$, and $P_T$ as functions of $\phi$ and evaluate them at $\phi = \phi_N$.
- Using the Markov Chain Monte Carlo(MCMC) package COSMOMC: we sample the following 8-dimensional set of cosmological parameters:
  - baryon and CDM densities, $\omega_b = \Omega_b h^2$ and $\omega_c = \Omega_c h^2$,
  - the ratio of the sound horizon to the angular diameter distance at decoupling, $\theta_s$,
  - the scalar spectral index, its running and the overall normalization of the spectrum, $n$, $dn/d\ln k$ and $A$ at $k = 0.002$ Mpc$^{-1}$,
  - the tensor contribution $r$, and, finally, the optical depth to reionization, $\tau$.

# Analysis Method

- In addition CMB data, we also consider the constraints on the real-space power spectrum of galaxies from the Sloan Digital Sky Survey (SDSS).
  - We restrict the analysis to a range of scales over which the fluctuations are assumed to be in the linear regime ($k < 0.2h^{-1}\mathrm{Mpc}$).
  - When combining the matter power spectrum with CMB data, we marginalize over a bias $b$ considered as an additional nuisance parameter.
- Furthermore, we make use of the HST measurement of the Hubble parameter $H_0 = 100h$ km s$^{-1}$Mpc$^{-1}$ by multiplying the likelihood by a Gaussian likelihood function centered around $h = 0.72$ and with a standard deviation $\sigma = 0.08$.
- Finally, we include a top-hat prior on the age of the universe: $10 < t_0 < 20$ Gyrs.

# Observational constraints from WMAP and SDSS

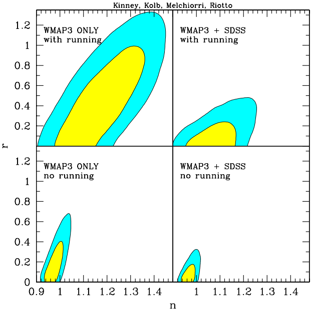


Constrints on the n-r plane

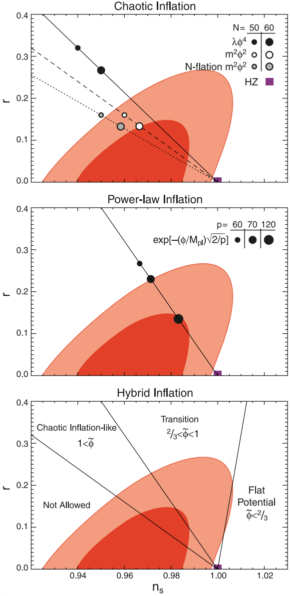


WMAP-5yr data

**Table:** One-dimensional confidence limits on inflationary parameters, marginalized over all other parameters, for WMAP3 alone and WMAP3 + SDSS.

| no running/ running | limits on $n$, $r$ 95% C.L. | data set |
|---|---|---|
| no running | $0.94 < n < 1.04$ | WMAP3 ONLY |
| | $r < 0.60$ | WMAP3 ONLY |
| | $0.93 < n < 1.01$ | WMAP3 + SDSS |
| | $r < 0.31$ | WMAP3 + SDSS |
| running | $1.02 < n < 1.38$ | WMAP3 ONLY |
| | $r < 1.09$ | WMAP3 ONLY |
| | $-0.17 < dn/d\ln k < -0.02$ | WMAP3 ONLY |
| | $0.97 < n < 1.21$ | WMAP3 + SDSS |
| | $r < 0.38$ | WMAP3 + SDSS |
| | $-0.13 < dn/d\ln k < 0.007$ | WMAP3 + SDSS |

# Observational constraints from WMAP and SDSS

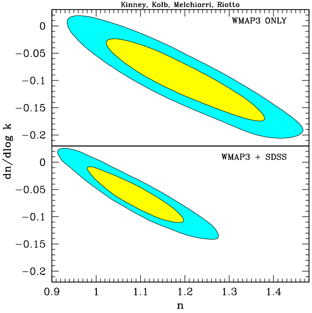


Constrints on the n-$dn/dlnk$ plane

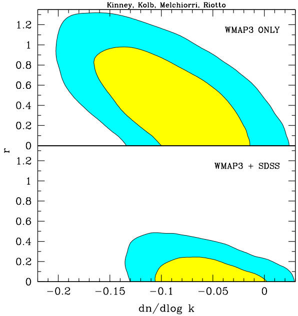


Constraint on the $dn/dlnk$-r plane

# Observational constraints from WMAP and SDSS

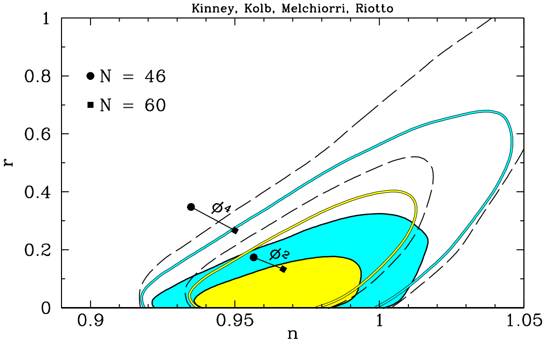


Figure: The $n$,$r$ parameter space WMAP3 alone (open contours) and WMAP3 + SDSS (filled contours), with a prior of $dn/d\ln k = 0$. The line segments show the predictions for $V(\phi) = m^2\phi^2$ and $V(\phi) = \lambda\phi^4$ for $N = [46, 60]$. The dashed lines show the 68% C.L. and 95% C.L. contours from the chains made public by the WMAP team, which do not include an HST prior on $H_0$ or an age prior.

# Numerical results from WMAP and SDSS

Figure: A representative sampling of reconstructed potentials lying within $|\Delta p| \leq 0.01$ of the best-fit model. The potentials are colored-coded according to their predicted values for $r$ at $k = 0.002\, h\mathrm{Mpc}^{-1}$: red yield $r \sim \mathcal{O}(10^{-1})$ and black yield $r < \mathcal{O}(10^{-1})$. The potentials have been given a common, arbitrary normalization at $\phi = 0$, when scales corresponding to the quadrupole exit the horizon.

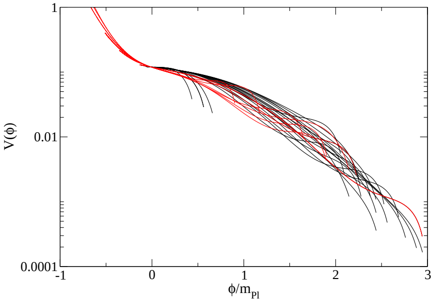

# Numerical results from WMAP and SDSS

| Parameter | $n = 1$ | $n = 2$ | $n = 3$ |
|---|---|---|---|
| $\Omega_b h^2$ | $0.023 \pm 0.001$ | $0.023 \pm 0.001$ | $0.022 \pm 0.001$ |
| $\Omega_{cdm} h^2$ | $0.109 \pm 0.004$ | $0.109 \pm 0.004$ | $0.110 \pm 0.004$ |
| $\theta$ | $1.042 \pm 0.003$ | $1.041 \pm 0.004$ | $1.040 \pm 0.004$ |
| $\tau$ | $0.08 \pm 0.03$ | $0.08 \pm 0.03$ | $0.09 \pm 0.03$ |
| $\ln\left[\frac{4H_*^4}{H_*'^2 m_P^6} 10^{10}\right]$ | $3.07 \pm 0.06$ | $3.07 \pm 0.06$ | $3.09 \pm 0.06$ |
| $\left(\frac{H_*'}{H_*}\right)^2 m_P^2$ | $0.079 \pm 0.031$ | $0.072 \pm 0.056$ | $0.081 \pm 0.067$ |
| $\frac{H_*''}{H_*} m_P^2$ | 0 | $-0.035 \pm 0.199$ | $-0.079 \pm 0.247$ |
| $\frac{H_*'''}{H_*} \frac{H_*'}{H_*} m_P^4$ | 0 | 0 | $1.53 \pm 1.23$ |
| $-\ln \mathcal{L}_{\max}$ | 1781.7 | 1781.4 | 1780.1 |

Table: Bayesian 68% confidence limits for ΛCDM inflationary models with a Taylor expansion of $H(\phi - \phi_*)$ at order $n = 1, 2, 3$ (with the primordial spectra computed numerically). The last line shows the maximum likelihood. The first four parameters have standard definitions (from Lesgourgues, Starobinsky and Valkenburg:2008).

# Numerical res

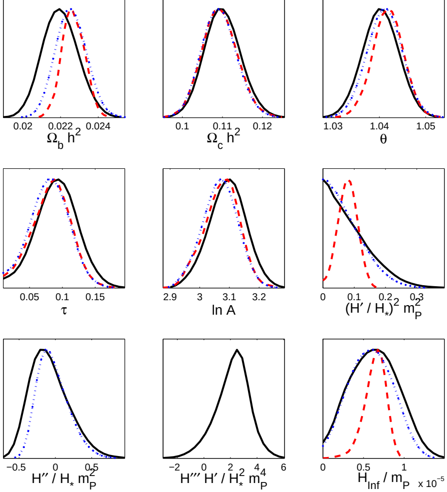


Figure: Probability distribution for the eight independent parameters of the models considered here, normalized to a common arbitrary value of $\mathcal{P}_{\max}$. The ninth plot shows a related parameter (with non-flat prior): namely, the value of the expansion rate when the pivot scale leaves the horizon during inflation. Our three runs $n = 1, 2, 3$ correspond respectively to the dashed red, dotted blue and solid black lines. The data consists of the WMAP 3-year results and the SDSS LRG

# Constraints on Single-field Slow-roll inflation

Constraints are becoming tighter: Single-field models may be excluded in the near future.

Multi-field models ? Non-Gaussiantity ?

- Tensor perturbations (gravitational waves) have not been detected yet.
  tensor-scalar ratio: r < 0.2 (95% C.L.)
  [WMAP+BAO+SN('08)]
- Future CMB experiments may detect non-Gaussianity (PLANCK):
  Gravitational potnetial: $\Phi = \Phi_{gauss} + f_{NL}\Phi^2_{gauss} + \ldots.$
  $-9 < f_{NL} < 111$(95% CL) [WMAP 5yr ('08)]

Fluctuations are Gaussian for single-field slow-roll inflation ....... marginally consistent with observation.

For beyond the single-field slow-roll inflation model,
See the poster by Dr. Pravabati Chingangbam.